IEEE Access
Multidisciplinary | Rapid Review | Open Access Journal

Received 16 October 2023, accepted 19 December 2023, date of publication 21 December 2023,
date of current version 3 January 2024.

Digital Object Identifier 10.1109/ACCESS.2023.3345803

RESEARCH ARTICLE

Chaotic Equilibrium Optimizer-Based Green Communication With Deep Learning Enabled Load Prediction in Internet of Things Environment

MOHAMMED ALJEBREEN[1], MARWA OBAYYA[2], HANY MAHGOUB[3], SAUD S. ALOTAIBI[4], ABDULLAH MOHAMED[5], AND MANAR AHMED HAMZA[6]

[1]Department of Computer Science, Community College, King Saud University, P.O. Box 28095, Riyadh 11437, Saudi Arabia
[2]Department of Biomedical Engineering, College of Engineering, Princess Nourah bint Abdulrahman University, P.O. Box 84428, Riyadh 11671, Saudi Arabia
[3]Department of Computer Science, College of Science & Art at Mahayil, King Khalid University, Abha 62529, Saudi Arabia
[4]Department of Information Systems, College of Computing and Information Systems, Umm Al-Qura University, Makkah 24382, Saudi Arabia
[5]Research Centre, Future University in Egypt, New Cairo 11845, Egypt
[6]Department of Computer and Self Development, Preparatory Year Deanship, Prince Sattam bin Abdulaziz University, Al-Kharj 16278, Saudi Arabia

Corresponding author: Manar Ahmed Hamza (ma.hamza@psau.edu.sa)

The authors extend their appreciation to the Deanship of Scientific Research at King Khalid University for funding this work through large group Research Project under grant number (RGP2/95/44). Princess Nourah bint Abdulrahman University Researchers Supporting Project number (PNURSP2023R203), Princess Nourah bint Abdulrahman University, Riyadh, Saudi Arabia. Research Supporting Project number (RSP2023R459), King Saud University, Riyadh, Saudi Arabia. This study is supported via funding from Prince Sattam bin Abdulaziz University project number (PSAU/2023/R/1444). This study is partially funded by the Future University in Egypt (FUE).

ABSTRACT Currently, there is an emerging requirement for applications related to the Internet of Things (IoT). Though the capability of IoT applications is huge, there are frequent limitations namely energy optimization, heterogeneity of devices, memory, security, privacy, and load balancing (LB) that should be solved. Such constraints must be optimised to enhance the network's efficiency. Hence, the core objective of this study was to formulate the intelligent-related cluster head (CH) selection method to establish green communication in IoT. Therefore, this study develops a chaotic equilibrium optimizer-based green communication with deep learning-enabled load prediction (CEOGC-DLLP) in the IoT environment. The study recognizes the emerging need for IoT applications and acknowledges the critical challenges, such as energy optimization, device heterogeneity, memory constraints, security, privacy, and load balancing, which are essential to enhancing the efficiency of IoT networks. The presented CEOGC-DLLP technique mainly accomplishes green communication via clustering and future load prediction processes. To do so, the presented CEOGC-DLLP model derives the CEOGC technique with a fitness function encompassing multiple parameters. In addition, the presented CEOGC-DLLP technique follows the deep belief network (DBN) model for the load prediction process, which helps to balance the load among the IoT devices for effective green communication. The experimental assessment of the CEOGC-DLLP technique is performed and the outcomes are investigated under different aspects. The comparison study represents the supremacy of the CEOGC-DLLP method compared to existing techniques with a maximum throughput of 64662 packets and minimum MSE of 0.2956.

INDEX TERMS Internet of Things, green communication, load prediction, clustering process, equilibrium optimizer.

I. INTRODUCTION

In recent times, revolutionary growth in IoT gadgets has opened the pattern for dynamic sensing technologies which render transmission across the Internet seamlessly [1]. Wireless sensor networks (WSNs) can be mostly utilized for collecting data and transmitting them over the 5G and beyond the 5G IoT network envisaged as 6G technology. Furthermore, the integration of IoT into WSNs will have several potentialities in numerous applications namely military,

The associate editor coordinating the review of this manuscript and approving it for publication was Giovanni Pau.

precision agriculture, health care, environment anomalies, smart cities, environment intelligent transport systems, and human intrusion detection and habitat monitoring [2]. But with all such noteworthy properties, the fallout in the lower lifespan of battery-enabled IoT gadgets and the unbalanced power consumption will limit the seamless interaction of intellectual gadgets across IoT networks [3]. Thus, energy-efficient transmission over 5G and beyond 5G (6G) assisted IoT gadgets is the primary consideration in IoT systems. Clustering can be referred to as a strong and scalable method to lesser power consumption having superior network throughput. It can be broadly learned as heuristic-based, probability-based, and weight-based techniques for conserving network energy [4]. Also, uncertainties and local decisions of the network dynamics have a massive effect on power utilization in the optimal selection of cluster head (CH) as nominated data forwarder [5]. Additionally, the issue of CH selection was non-deterministic polynomial hard (NP) as optimum data aggregation is not proficiently resolved in the polynomial period for ensuring balanced power utilization in each round by making use of weight- and probability-based techniques [6].

The ideas of hierarchical routing were enforced to achieve energy efficiency in WSNs. Conversely, lower power nodes will be employed for sensor-based work in regions which were closer to the target. So, allocating specific jobs to CHs could prominently contribute to the system's scalability, its power efficiency, and its lifetime [7]. Scalability will be considered to be a serious aspect of WSNs and it is not accomplished well in several protocols because of initial assumptions. For instance, cluster-related protocol usually takes a single sink with CHs into account inside the sink coverage [8]. Under such considerations, WSNs lack scalability and lead to transmissions that are disproportionate to their power necessities. Later, slightly raising the width of the network or the number of device nodes would result in overloading that progresses aggressively, and a difficulty that has just one sink; these could hamper the network. Hierarchical routing was a potential means to reduce power utility within the cluster and execute data accumulation [9]. Along with this, this method would allow the integration of tasks for decreasing the count of transported packets to sink. Every perception of the nodes, from hardware gadgets to their established process, would be helpful in dispensing power load. However numerous communication modes, like normal sensors and CHS, will be beneficial if enforced in every layer [10].

This study develops a chaotic equilibrium optimizer-based green communication with deep learning-enabled load prediction (CEOGC-DLLP) in the IoT environment. The presented CEOGC-DLLP technique mainly accomplishes green communication via clustering and future load prediction processes. To do so, the presented CEOGC-DLLP model derives the CEOGC technique with a fitness function (FF) encompassing multiple parameters. In addition, the presented CEOGC-DLLP technique follows the deep belief network (DBN) model for the load prediction process, which helps to balance the load among the IoT devices for effective green communication. The experimental assessment of the CEOGC-DLLP technique was executed and the outcomes were examined under several aspects.

II. RELATED WORKS

In [11], the author endeavours to maximize the energy consumption in the IoT network by selecting optimal CH utilizing a recently advanced nature-inspired technique called the Harris Hawks Optimization algorithm (HHO). The HHO-oriented CH method's performance can be scrutinized with the help of numerous metrics like load, delay, temperature, count of alive nodes, and residual energy. In [12], the authors solve the concern of green transmission in 6G-assisted enormous IoT gadgets through cluster-related data distribution in the network. The authors devise a new hybrid whale spotted hyena optimization (HWSHO) technique through the production of the WOA exploiting abilities of spotted hyena optimizer (SHO). Akhtar et al. [13] formulate the intelligent-related CH selection method to accomplish green transmission in IoT. The two well-known techniques such as sunflower optimization (SFO) and spotted hyena optimization (SHO) were compiled for making sunflower-spotted hyena optimization (SF-SHO) by using the hybrid meta-heuristic idea for selecting optimal CH.

Singh et al. [14] devise an optimized GA-related sustainable and secure green data transmission or collection technique for IoT-assisted WSN in the medical sector through optimization of intra-cluster distance, reducing hop count, and systematic use of node's energy. For secure communication of data, transmitting data was encoded with the help of a stream cipher and pseudo-randomly generated security key. Furthermore, the devised movable sink and data transmission or collection techniques curtail transmission distance between the sink and CH would diminish the hotspot problems. Rehman et al. [15] intend to devise a method of security measures utilizing the Green IoT including Cloud Integrated Data Management (M-SMDM) for Smart City. Initially, it would form energy-efficient and long-run connectivity by utilizing distributing load factors and self-balancing trees homogeneously in a green transmission mechanism. Then, it solves the issue of secret key distribution among peer nodes and achieves trust for both direct and partial interaction. Eventually, it secures transmission mechanisms from mobile gateways to users contrary to menaces with enhanced data latency and overheads.

Kumar et al. [16] modelled a quantum-based green communication structure for Energy Balancing in sensor-assisted IoT networks (Q-EBIoT). Firstly, an energy-optimized technique for sensor-assisted IoT atmospheres was offered, whereas power utilization was extracted as the cost of energy-based paths. Secondly, quantum computing-based solutions were formulated for optimized issues concentrating

on energy-centric solution representation, rotation angle, and measurement. Kaur et al. [17] presented a green hybrid congestion control system for IoT-assisted WSNs. It employs an unequal clustering system which would save power of battery-limited SNs and solve energy hole problems. Besides, an innovative 2-class priority-related congestion avoidance system was modelled which suggestively decreases transmission delay.

Zhang et al. [18] intend to improve small and medium-sized enterprises (SMEs) core competitiveness and financing attainability using the DL algorithm by economic globalization. Consequently, the study presents a supply chain symbiosis technique by using DL, economics, and Stackelberg game theory following a status quo analysis of the financing status of SMEs. Emroozi et al. [19] illustrate the capability of four dissimilar combinatorial multi-criteria decision-making (CMCDM) methods to determine the good supplier in the rubber GSC. In [20], an intelligent dynamic subarray RIS architecture is based on deep reinforcement learning (DRL). The main concept is to split RIS electromagnetic elements into different groups and power basic amplifier factors, and independent phase shifts to optimize and improve the system energy competence with the assumption of the user's requirement. Alandjani [21] introduces a review of patients' healthcare services., we first provide a summary of the crucial parameters of patients' healthcare services via Green-IoT-enabled sensor technology under the use case scenario.

A notable research gap in the context of green communication in the IoT environment lies in the incorporation of metaheuristic-based clustering and DL-based load prediction techniques. While metaheuristics and DL have individually illustrated their efficiency in enhancing IoT networks, there is a lack of research that explores their synergistic application in tandem. The incorporation of these techniques could provide a holistic method to address the energy efficacy and load balancing challenges in IoT systems. Research is needed to examine how these two paradigms can complement one another to accomplish better sustainability, resource allocation, and network performance in IoT, filling the present void in the literature and contributing to the development of green communication solutions in IoT.

III. THE PROPOSED MODEL

In this study, a new CEOGC-DLLP method was projected for green communication and load prediction in the IoT environment. The presented CEOGC-DLLP technique mainly accomplishes green communication via clustering and future load prediction processes. It encompasses a two-stage process namely cluster-based green communication and load prediction. Fig. 1 showcases the block diagram of the CEOGC-DLLP system.

A. DESIGN OF CEOGC TECHNIQUE

Primarily, the clustering of the IoT devices is performed using the CEOGC technique. The EO was presented in 2019 by Faramaezi et al. [22]. The motivation for the presented methodology is a modest mixed thoroughly dynamic mass balance on controller volume, wherein a mass balance formula is utilized for describing the application of non-reactive constituents in a controller volume as a task of numerous sink and source models and it can be explained in the subsequent equation.

$$V\frac{dC}{dt} = QC_{eq} - QC + G \tag{1}$$

In Eq. (20), V signifies the controller volume, C signifies the application of particles, $V\frac{dC}{dt}$ denotes the rate of change Q signifies the volumetric flow rate, C_{eq} denotes the application of particles at equilibrium state without generation and G denotes mass generative rate.

If $V\frac{dC}{dt} = 0$, a steady equilibrium state was accomplished. $\lambda = \frac{Q}{y}$ described the turnover rate, whereas $\frac{Q}{y}$ shows the inverse of the residence duration:

$$\frac{dC}{\lambda C_{eq} - \lambda C + \frac{G}{y}} = dt \tag{2}$$

The below formula demonstrates the incorporation of Eq. (2) over time.

$$\int_{C_0}^{C} \frac{dC}{\lambda C_{eq} - \lambda C + \frac{G}{y}} = \int_{t_0}^{t} dt. \tag{3}$$

The outcome is shown below

$$C = C_{eq} + \left(C_0 - C_{eq}\right)F + \frac{G}{\lambda V}\left(1 - F\right) \tag{4}$$

In Eq. (4), F is evaluated as follows

$$F = \exp\left(-\lambda\left(t - t_0\right)\right) \tag{5}$$

In Eq. (5), t_0 and C_0 characterize the primary time and concentration.

The EO approach creates the vector named equilibrium pool that gives equilibrium candidate particles. Five candidate particles of the equilibrium pool are defined using the study, the optimum particle recognized in the entire optimization technique, and the arithmetic mean of the above-mentioned four particles [23]. Four ideal particle helps to better examine the solution whereas the average assist in exploitation:

$$\vec{C}_{eq,pool} = \left\{\vec{C}_{eq(1)}, \vec{C}_{eq(2)}, \vec{C}_{eq(3)}, \vec{C}_{eq(4)}, \vec{C}_{eq(ave)}\right\}. \tag{6}$$

Exponential term F

Exponential term F aim is to balance the exploitation and exploration of the presented approach and it is calculated in the following:

$$F = e^{(-\lambda(t-t_0))} \tag{7}$$

In Eq. (7), λ indicates an arbitrary value within [0,1], *and* t denotes an iteration function that minimizes the iteration count:

$$t = (1 - \frac{Iter}{\mathrm{Max}_{iter}})^{\alpha_2 \frac{Itr}{\mathrm{Max}_{iter}}} \tag{8}$$

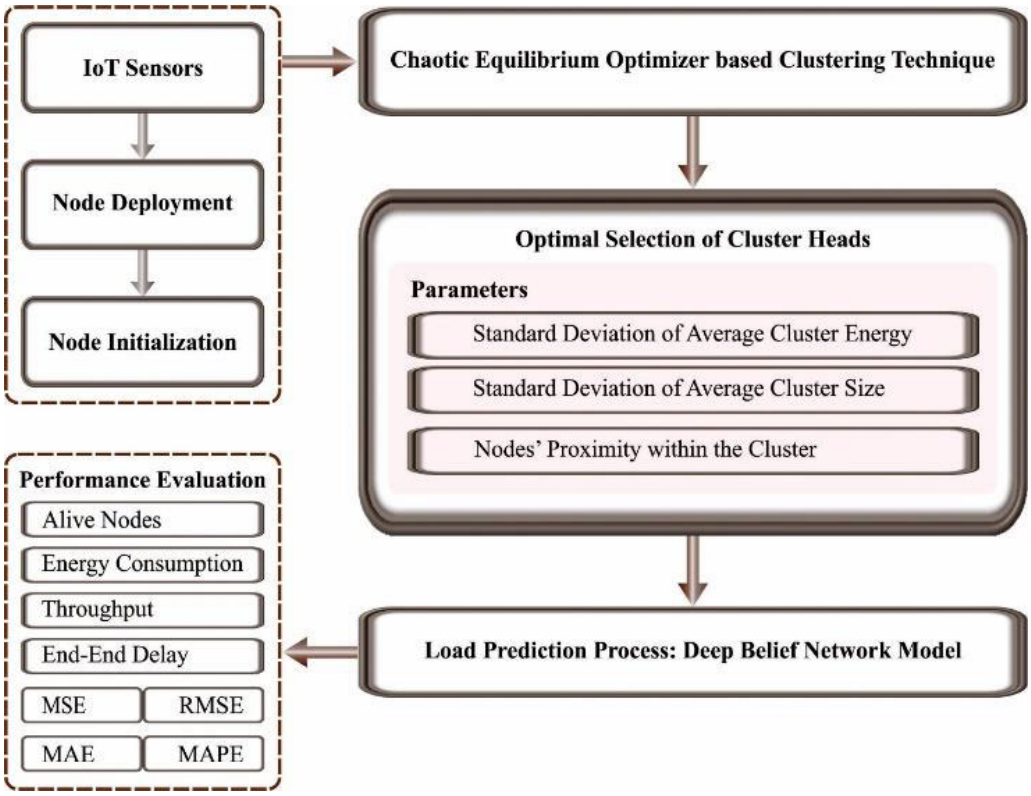

FIGURE 1. Block diagram of CEOGC-DLLP system.

In Eq. (8), Iter and Max_{iter} represent the present and the maxima amount of iterations, correspondingly:

$$\vec{t_0} = 1\vec{\lambda}\ln(-\alpha_1 sign(\vec{r} - 0.5)[1 - e^{-\lambda t}]) + t \tag{9}$$

whereas α_1 and α_2 indicate constant, and they control exploitation and exploration abilities, correspondingly. The high value of α_1, the strong exploration ability, and the worsening exploitation ability. The higher the value of α_2, the stronger the exploitation ability was and the worse the exploration ability. α_1 and α_2 are equivalent to 2 and 1, correspondingly. $sign(r - O.5)$ specifies the direction of exploitation and exploration.

$$\vec{F} = \alpha_1 sign(\vec{r} - 0.5)[e^{-\lambda\tau} \to -1]. \tag{10}$$

Generation rate G assurances the EO approach for providing precise solutions by enhancing the exploitation ability. Assume a first-order exponential decay procedure to determine the generative rate.

$$\vec{G} = \vec{G}_0 e^{-k(\vec{t} - t_0)} \tag{11}$$

In Eq. (11), $\vec{G}_0$ denotes the primary value; k represents a decay constant equivalent to λ. Consequently, the concluding expression of generative rate $\vec{G}$ is equivalent to λ.

$$\vec{G} = \vec{G}_0 e^{-\vec{k}\langle t - t_0\rangle} = \vec{G}_0\vec{F} \tag{12}$$

whereas

$$\vec{G} = GC\vec{P}\left(\vec{C}_{eq} - \vec{\lambda}\vec{C}\right) \tag{13}$$

$$G\tilde{C}P = \begin{cases} 0.5r_1, & r_2 \geq GF \\ 0, & r_2 < GF \end{cases} \tag{14}$$

Now, r_1 and r_2 indicate random numbers within [0,1], and $G\vec{C}P$ represents the likelihood that the generative term contributed to the updating procedure that is named the generative rate controller variable parameter; the probability of these contributions represents how much the particle uses generative terms to upgrade the state. $G\vec{C}F$ can be achieved based on Eq. (14), which is named the generative possibility, and its part is to accomplish a better balance between exploration and exploitation:

$$\frac{\vec{C} = \vec{C}_{eq} + (\vec{C}_0 - \vec{C}_{eq})\vec{F} + \vec{G}}{\vec{\lambda}V(1 - \vec{F})} \tag{15}$$

whereas V denoted the considered a unit.

The CEO algorithm was derived by the use of the chaotic concept. During the iteration process, the range and size of the early population have a substantial influence on the convergence speed and the solution quality. Meanwhile, the concentration and location of the optimum solution are unidentified initially, when the individual of the early population could be distributed consistently in the problem, it might efficiently increase the search efficacy. To get the best primary values of diversity, a chaotic mapping approach was applied for initializing the population.

Logistic mapping will be a direct chaotic mapping in an arithmetical format. This scheme has tremendously complicated dynamics and extensive application.

$$x_i^{k+1} = |1 - 2(x_i^k)^2| \tag{16}$$

whereas $x_i^k \in [0, 1]$ indicates the chaotic series: $k = 1, 2, \ldots, L, L$ represents the original population: $i = 1, 2 \ldots, N, N$ represents the early population number. Carrying out the mapping function to x_i^k attains the early population y_i^k of the problem, and it was evaluated in the following expression.

$$y_i^k = L_i + (U_i - L_i)\, x_i^k \tag{17}$$

In Eq. (17), L_i and U_i represent the boundary of parameter values.

The presented CEOGC-DLLP model derives the CEOGC technique with an FF encompassing multiple parameters. It is simply intuited that once the cluster is balanced in the cluster network, it may contain an approximately equivalent amount of member nodes and an equivalent level of RE [24]. Using these concepts, to satisfy the major goal of the network dividing into a few balanced clusters, nodes' RE and the size of the cluster are considered as decision parameters. Furthermore, nodes' proximity was considered, which ensures decreased energy consumption in intra-cluster transmission. An appropriate FF often contributes to differential evolution. Therefore, FF was derived so that it symbolizes the above-mentioned requirement in the following:

1) STANDARD DEVIATION (SD) OF AVERAGE CLUSTER ENERGY

If the cluster is optimally formed, ensuring that the whole network energy is evenly dispersed over the cluster in a network, all the clusters should have an approximately equivalent level of RE. In other words, it is demonstrated that concerning average cluster energy (ACE), every cluster must have an almost similar quantity of energy, and therefore, SD is shown below:

$$\sigma_{CE} = \sqrt{\frac{1}{k} * \sum_{i=1}^{k} (ACE - Cluster_{RE}^i)^2} \tag{18}$$

In Eq. (18), k represents the cluster count. It is rather noticeable that low the value of σ_{CE}, the high value of fitness, is shown below

$$FitnessValue \propto \frac{1}{\sigma_{CE}}. \tag{19}$$

2) SD OF AVERAGE CLUSTER SIZE

The balanced cluster should have an almost equivalent amount of members. In other words, it is demonstrated that the average cluster size (AvgCS) of all the clusters is approximately a similar amount of cluster members. The fitness value and SD are shown as follows.

$$\sigma_{cs} = \sqrt{\frac{1}{k} * \sum_{i=1}^{k} (AvgCS - CS_i)^2}, \tag{20}$$

In Eq. (20), k represents the cluster count. It is perceived again that the lower the value of σ_{cs}, the higher the value of fitness as

$$Fitness\ Value \propto \frac{1}{\sigma_{cs}}. \tag{21}$$

3) NODES' PROXIMITY WITHIN A CLUSTER

This was a metric that guarantees that while deciding on the node that part of clusters, the one positioned at a short distance from another member gets priority.

$$Fitness\ Value \propto \frac{1}{\sum_{m=1}^{k} dist_m\,(i, j)}. \tag{22}$$

From Eqs. (19), (21), and (22), it is written as:

$$Fitness\ Value \propto \frac{1}{\sigma_{CE}} * \frac{1}{\sigma_{cs}} * \frac{1}{\sum_{m=1}^{k} dist_m\,(i, j)}, \tag{23}$$

viz.,

$$Fitness\ Value = \frac{\mathrm{K}}{\sigma_{CE} * \sigma_{cs} * \sum_{m=1}^{k} dist_m(i, j)}, \tag{24}$$

From the expression, K'' is *apropor* tionality constant that is set to $K = 1$ without losing generality.

Thus, (25), as shown at the bottom of the next page, or (26), as shown at the bottom of the next page.

B. LOAD PREDICTION USING DBN MODEL

In this work, the presented CEOGC-DLLP technique follows the DBN model for the load prediction process, which helps to balance the load among the IoT devices for effective green communication [25]. The DBN model training can be classified as follows: unsupervised pre-training procedure depends on RBM and supervised parameter adjustment technique. The primary input layer was the visible layer (VL), and the input dataset was the text feature vector. The vector data of VL v integrated to weight w_1 is utilized for inferring the data vector of the hidden layer (HL) h_1 which is the training procedure of RBM1. Next, the vector data of the HL h_1 is integrated to weight w_2 for inferring the vector data of HL h_2 which is the training procedure of RBM2, etc. The pretraining procedure of DBN is accomplished:

Step 1. Arbitrarily initializing the weight (W, a, b), where W indicates the weight vector matrixes, $a = [a_1, a_2, \ldots, a_n]$ denotes the offset coefficient of VL, and $b = [b_1, b_2, \ldots, b_n]$ shows the offset coefficient of HL. $v = [v_1, v_2, \ldots, v_n]$ represent visible neuron, number is n;$h = [h_1, h_2, \ldots, h_n]$ denotes hidden neuron, number is m. Fig. 2 illustrates the infrastructure of DBN.

Step 2. Allocate X value to VL $v^{(0)}$ and evaluate the probability that the hidden neuron is activated:

$$p\left(h_j^{(0)} = 1 \mid v^{(0)}\right) = \sigma\left(W_j * v^{(0)} + b_j\right). \tag{27}$$

Step 3. Execute a Gibbs sampling to achieve the values of all the neurons in HL:

$$h^{(0)} \sim p\left(h^{(0)} \mid v^{(0)}\right). \tag{28}$$

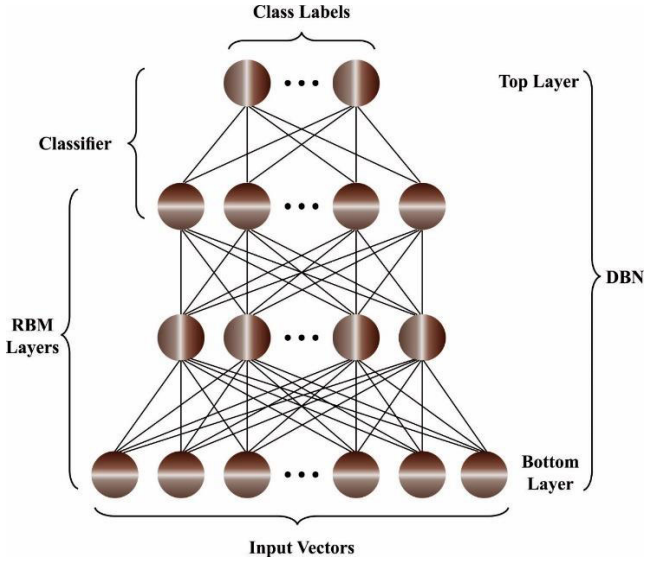

FIGURE 2. Architecture of DBN.

Step 4. Recreate the VL v with gained $h^{(0)}$ in Eq. (28) and evaluate the likelihood density:

$$p\left(v_i^{(0)} = 1 \mid h^{(0)}\right) = \sigma\left(W_i * h^{(0)} + a_i\right). \tag{29}$$

Step 5. Implement Gibbs sampling again and recreate the value of all the neurons in the VL. Let $r_i \in$ random of zero and one:

$$v_i = \begin{cases} 1, & p\left(v_i^{(0)} = 1. \mid h^{(0)}\right) > r_i, \\ 0, & \text{otherwise} \end{cases} \tag{30}$$

Step 6. Evaluate the activation probability of HL neurons again with recreated VLs:

$$p\left(h_j^{(1)} = 1 \mid v^{(1)}\right) = \sigma\left(W_j * v^{(1)} + b_j\right), \tag{31}$$

In Eq. (31), σ adopted the sigmoid activation function. Sigmoid is utilized for activating the function since it is description field is R and it is value field is $(0, 1)$. Consequently, the input data of neurons in VL was the activation likelihood of node attained using a sigmoid function.

Step 7. Attain the novel weighted vector matrixes W, VL offset co-efficient a, and HL offset co-efficient b:

$$a = a + \varepsilon[v^{(0)} - v^{(1)}],$$
$$b = b + \varepsilon[p(h^{(0)} = 1|v^{(0)}) - p(h^{(1)} = 1|v^{(1)})],$$

TABLE 1. NOAN analysis of CEOGC-DLLP algorithm with recent systems under 300 nodes.

No. of Alive Nodes; No. of Nodes (300)					
No. of Rounds	F-LEACH	EE-FUC	UDCH	GEQCC-FLP	CEOGC-DLLP
500	300	300	300	300	300
1000	223	262	287	295	299
1500	139	225	264	281	299
2000	76	170	205	240	290
2500	40	101	145	203	271
3000	15	33	53	92	201

$$W = W + \varepsilon\left[p\left(h^{(0)} = 1 \mid v^{(0)}\right) v^{(0)T} - p\left(h^{(1)} = 1 \mid v^{(1)}\right) v^{(1)T}\right], \tag{32}$$

whereas ε indicates the learning rate.

To add, pre-training requires iteratively evaluating RBM1, RBM2, and RBM3 variables sequentially and lastly getting a better weight (W, a, b).

The supervised parameter optimization training of DBN firstly makes use of the forwarding propagation technique for determining whether the HLs are activated through the parameters W and b attained. Consider l indicates the layer count of the NN and evaluate the excitation value of all the HLs:

$$h^{(l)} = W^{(l)} * v + b^{(l)}. \tag{33}$$

Next, disseminate upward layer-wise, compute the excitation value of neurons in HL, normalize them with activation function, and lastly evaluate excitation values $h^{(l)}$ and output vector $\hat{X}$ of output layer:

$$h^{(l)} = W^{(l)} * h^{(l-1)} + b^{(l)},$$
$$\hat{X} = f(h^{(l)}). \tag{34}$$

Next, the backpropagation model is utilized for updating the parameters of the entire DBN network. The backpropagation model adopts the reconstructed errors, and the cost function is given below:

$$E = \frac{1}{N}(\hat{X}(W^{(l)}, b^{(l)}) - X_i)^2, \tag{35}$$

In Eq. (35), E refers to the reconstructed error, $\hat{X}$ indicates the actual outcome of the resultant layer, X_i represents the theoretical output belonging to the output layer, and $(W^{(l)}, b^l)$

$$Fitness\ Value = \frac{1}{\sqrt{1/k * \sum_{i=1}^{k}(ACE - Cluster_{RE}^{i})^2} * \sqrt{1/k * \sum_{i=1}^{k}(AvgCS - CS_i)^2} * \sum_{m=1}^{k} dist_m(i,j)} \tag{25}$$

$$Fitness\ Value = \frac{k}{\sqrt{\sum_{i=1}^{k}(ACE - Cluster_{RE}^{i})^2} * \sqrt{\sum_{i=1}^{k}(AvgCS - CS_i)^2} * \sum_{m=1}^{k} dist_m(i,j)} \tag{26}$$

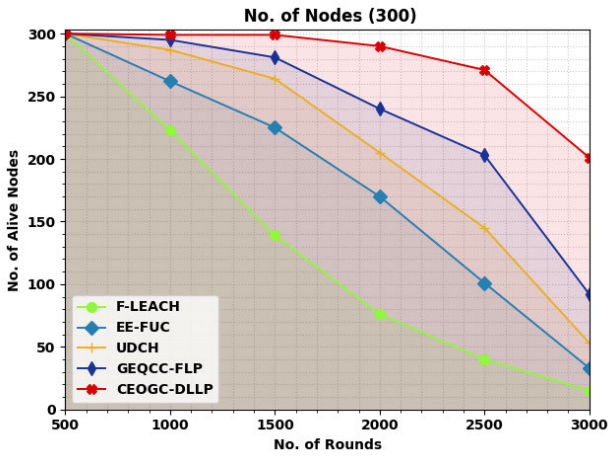

FIGURE 3. NOAN analysis of CEOGC-DLLP algorithm under 300 nodes.

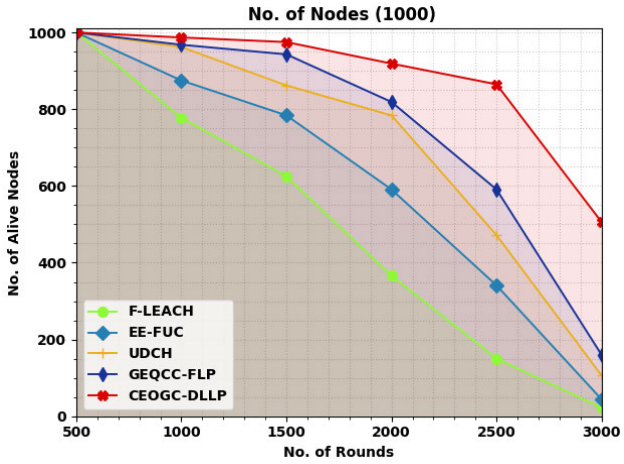

FIGURE 4. NOAN analysis of CEOGC-DLLP algorithm under 1000 nodes.

TABLE 2. NOAN analysis of CEOGC-DLLP algorithm with recent systems under 1000 nodes.

No. of Alive Nodes; No. of Nodes (1000)					
No. of Rounds	F-LEACH	EE-FUC	UDCH	GEQCC-FLP	CEOGC-DLLP
500	1000	1000	1000	1000	1000
1000	778	875	962	968	987
1500	625	784	862	943	975
2000	366	591	784	819	919
2500	150	341	472	591	865
3000	22	44	106	160	506

TABLE 3. ECOM analysis of CEOGC-DLLP algorithm with recent systems under varying rounds.

Energy Consumption (J)					
No. of Rounds	F-LEACH	EE-FUC	UDCH	GEQCC-FLP	CEOGC-DLLP
500	55	45	40	24	21
1000	74	57	42	32	24
1500	89	67	51	37	29
2000	95	77	60	51	36
2500	100	91	77	70	44
3000	100	99	98	93	84

signifies the weighted and offset co-efficient of layer l. The reconstructed error reflects the probability of the trained dataset to a specific range.

$$\left(W^{(l)}, b^{(l)}\right) = \left(W^{(l)}, b^{(l)}\right) - \varepsilon \frac{\partial E}{\partial \left(W^{(l)}, b^{(l)}\right)}. \quad (36)$$

The training objective of DBN was to exploit the fitting of the input dataset, and the output was the reconstructed error of the trained dataset. The VL neuron transfers its features to HLs. The HLs capture the high-level feature demonstrated using the VLs via iterative training, for improving the capability of feature extraction.

IV. RESULTS AND DISCUSSION

In this section, the green communication and load prediction outcomes of the CEOGC-DLLP model are investigated briefly. Table 1 and Fig. 3 offer a NOAN inspection of the CEOGC-DLLP model with recent models under 300 nodes. These results inferred the enhanced outcomes of the CEOGC-DLLP model with increased NOAN values. For instance, on 1000 rounds, the CEOGC-DLLP model has attained an increased NOAN of 299 whereas the F-LEACH, EE-FUC, UDCH, and GEQCC-FLP models have reached reduced NOAN of 223, 262, 287, and 295 respectively. Besides, on 3000 rounds, the CEOGC-DLLP method has achieved an increased NOAN of 201 whereas the F-LEACH, EE-FUC, UDCH, and GEQCC-FLP approaches have reached reduced NOAN of 15, 33, 53, and 92 respectively.

Table 2 and Fig. 4 render a NOAN review of the CEOGC-DLLP approach with recent techniques under 1000 nodes. These results denoted the enhanced outcomes of the CEOGC-DLLP approach with increased NOAN values. For example, on 1000 rounds, the CEOGC-DLLP technique has achieved an increased NOAN of 987 whereas the F-LEACH, EE-FUC, UDCH, and GEQCC-FLP approaches have reached reduced NOAN of 778, 875, 962, and 968 correspondingly. Also, on 3000 rounds, the CEOGC-DLLP technique has obtained an increased NOAN of 506 whereas the F-LEACH, EE-FUC, UDCH, and GEQCC-FLP models have reached reduced NOAN of 22, 44, 106, and 160 correspondingly.

Table 3 and Fig. 5 inspect the ECOM examination of the CEOGC-DLLP model with existing techniques. The results represented that the CEOGC-DLLP model obtained reduced ECOM values under all rounds. For instance, on 1000 rounds, the CEOGC-DLLP model has reached a minimal ECOM of 21J whereas the F-LEACHEE-FUC, UDCH, and GEQCC-FLP models have attained maximum ECOM values of 55J, 45J, 40J, and 24J respectively. Besides, on 3000 rounds, the CEOGC-DLLP technique has reached a minimal ECOM of 84J whereas the

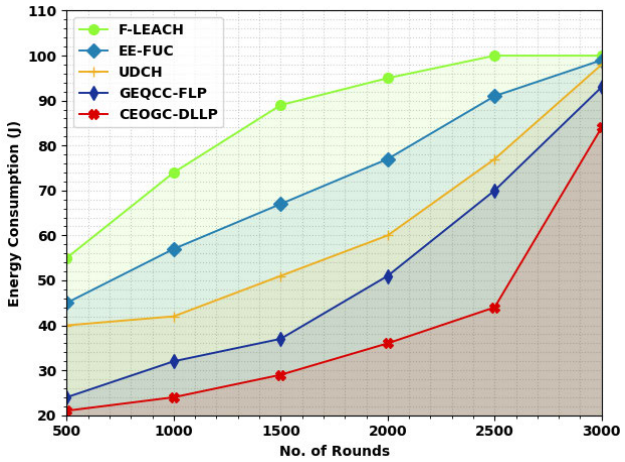

FIGURE 5. ECOM analysis of CEOGC-DLLP algorithm under varying rounds.

TABLE 4. ETED analysis of CEOGC-DLLP algorithm with recent systems under varying rounds.

End-to-End Delay (ms)					
No. of Rounds	F-LEACH	EE-FUC	UDCH	GEQCC-FLP	CEOGC-DLLP
500	32	24	20	11	5
1000	37	31	25	16	9
1500	41	35	28	19	11
2000	43	36	29	22	15
2500	47	37	31	27	19
3000	49	39	33	26	19

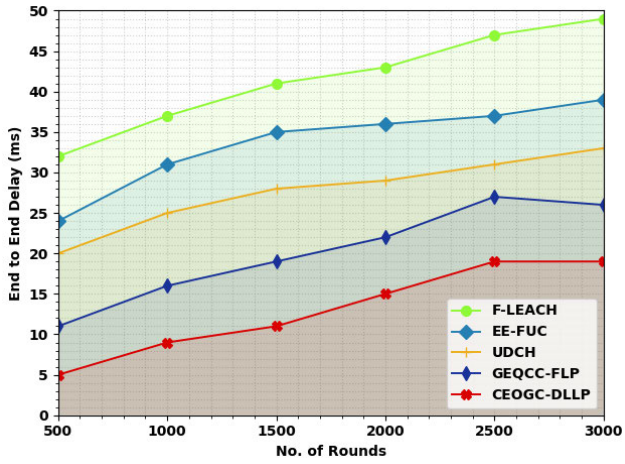

FIGURE 6. ETED analysis of CEOGC-DLLP algorithm under varying rounds.

F-LEACHEE-FUC, UDCH, and GEQCC-FLP approaches have reached maximum ECOM values of 100J, 99J, 98J, and 93J correspondingly.

Table 4 and Fig. 6 review the ETED inspection of the CEOGC-DLLP method with existing methods. The results signified the CEOGC-DLLP approach procured reduced ETED values under all rounds. For example, on 1000 rounds, the CEOGC-DLLP technique has attained a minimal ETED of 9ms whereas the F-LEACHEE-FUC, UDCH, and GEQCC-FLP approaches have obtained maximum ETED values of 37ms, 31ms, 25ms, and 16ms correspondingly. Also, on 3000 rounds, the CEOGC-DLLP technique has attained a minimal ETED of 19ms whereas the F-LEACHEE-FUC, UDCH, and GEQCC-FLP algorithms have reached maximum ETED values of 49ms, 39ms, 33ms, and 26ms correspondingly.

TABLE 5. Throughput analysis of CEOGC-DLLP algorithm with recent systems under varying rounds.

Throughput (Pkts)					
No. of Rounds	F-LEACH	EE-FUC	UDCH	GEQCC-FLP	CEOGC-DLLP
500	16750	17711	19634	21397	23640
1000	18512	20756	23480	29569	34216
1500	21236	25403	29088	35177	41747
2000	26364	29889	35338	41267	47356
2500	29248	37261	43670	49599	54246
3000	36940	44632	51362	57451	64662

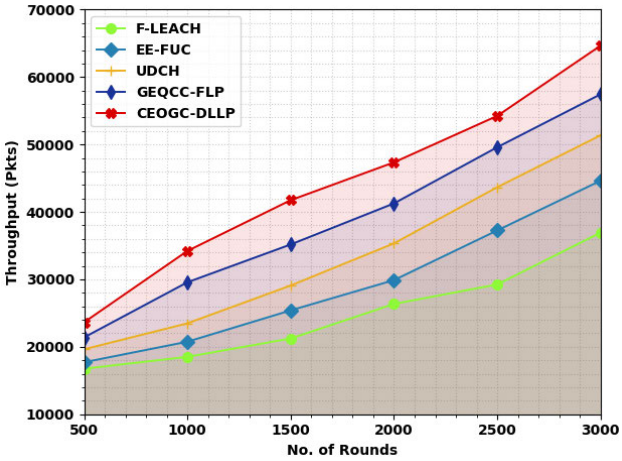

FIGURE 7. Throughput analysis of the CEOGC-DLLP algorithm under varying rounds.

TABLE 6. Comparative analysis of CEOGC-DLLP algorithm with recent systems.

Methods	MSE	RMSE	MAE	MAPE
LR Model	0.3240	0.5692	0.4774	0.1545
LSTM Model	0.6080	0.7797	0.6538	0.2377
CNN-LSTM Model	0.3940	0.6277	0.4932	0.2106
GRU-LSTM Model	0.3430	0.5857	0.4535	0.1946
GEQCC-FLP	0.3210	0.5666	0.4413	0.1356
CEOGC-DLLP	0.2956	0.5437	0.4028	0.1163

Table 5 and Fig. 7 offer a throughput (THRO) examination of the CEOGC-DLLP technique with recent models under 1000 nodes. These results inferred the enhanced outcomes of the CEOGC-DLLP methodology with increased THRO values. For example, on 1000 rounds, the CEOGC-DLLP technique has reached an increased THRO of 34216Pkts whereas the F-LEACH, EE-FUC, UDCH, and GEQCC-FLP techniques have reached a reduced THRO of 18512Pkts, 20756Pkts, 23480Pkts, and 29569Pkts correspondingly.

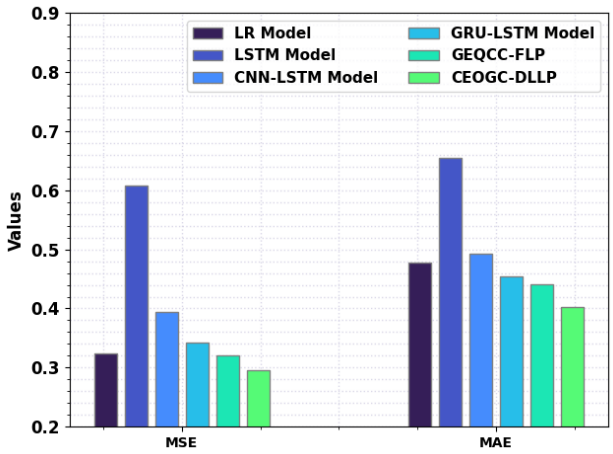

FIGURE 8. MSE and MAE analysis of CEOGC-DLLP algorithm with recent systems.

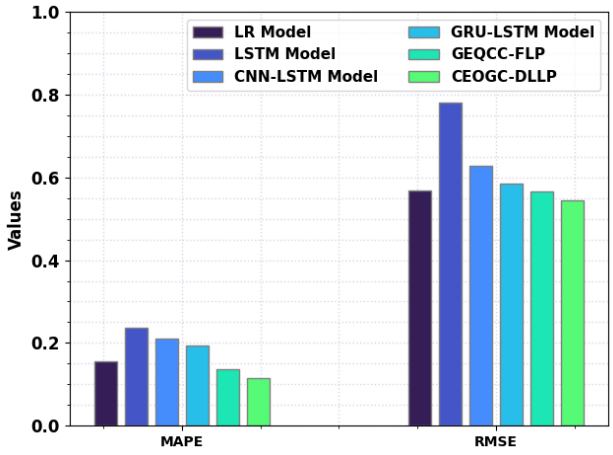

FIGURE 9. RMSE and MAPE analysis of CEOGC-DLLP algorithm with recent systems.

Also, on 3000 rounds, the CEOGC-DLLP algorithm has attained increased THRO of 64662Pkts whereas the F-LEACH, EE-FUC, UDCH, and GEQCC-FLP approaches have attained reduced THRO of 36940Pkts, 44632Pkts, 51362Pkts, and 64662Pkts correspondingly.

Table 6 provides comparative load prediction results of the CEOGC-DLLP model [2]. Fig. 8 shows the MSE and MAE assessment of the CEOGC-DLLP with existing models. The figure reported that the CEOGC-DLLP model outperformed the other models with minimal values of MSE and MAE. Based on MSE, the CEOGC-DLLP model has reached a minimal MSE of 0.2956 whereas the LR, LSTM, CNN-LSTM, and GEQCC-FLP models have attained maximum MSE of 0.3240, 0.6080, 0.3940, 0.3430, and 0.3210 respectively. At the same time, based on MAE, the CEOGC-DLLP method has reached a minimal MAE of 0.1028 whereas the LR, LSTM, CNN-LSTM, and GEQCC-FLP techniques have reached a maximum MAE of 0.4774, 0.6538, 0.4932, 0.4535, and 0.4413 correspondingly.

Fig. 9 displays the RMSE and MAPE valuation of the CEOGC-DLLP with existing techniques. The figure reported that the CEOGC-DLLP method outperformed the other models with minimal values of RMSE and MAPE. Based on RMSE, the CEOGC-DLLP technique has reached a minimal RMSE of 0.5437 whereas the LR, LSTM, CNN-LSTM, and GEQCC-FLP methodologies have obtained a maximum RMSE of 0.5692, 0.7797, 0.6277, 0.5857, and 0.5666 correspondingly.

Simultaneously, based on MAPE, the CEOGC-DLLP technique has reached a minimal MAPE of 0.1163 whereas the LR, LSTM, CNN-LSTM, and GEQCC-FLP approaches have gained a maximum MAPE of 0.1545, 0.2377, 0.2106, 0.1946, and 0.1356 correspondingly. These results assured the promising performance of the CEOGC-DLLP model.

V. CONCLUSION

In this study, a new CEOGC-DLLP technique has been developed for green communication and load prediction in the IoT environment. The presented CEOGC-DLLP technique mainly accomplishes green communication via clustering and future load prediction processes. The CEOGC-DLLP technique has shown remarkable promise in addressing the critical challenges of energy optimization, load balancing, and overall network efficiency in the IoT environment. By combining the power of metaheuristic-based clustering with DL-based load prediction, this approach offers a comprehensive solution to enhance sustainability and resource allocation. The experimental assessment of the CEOGC-DLLP technique is performed and the results are investigated under several aspects. The comparison study represents the supremacy of the CEOGC-DLLP technique compared to existing techniques with a maximum throughput of 64662packets and minimum MSE of 0.2956. In future, the proposed load prediction can be extended to long-term forecasting for supporting strategic planning, capacity management, and infrastructure development in the IoT environments. In future work, the CEOGC-DLLP approach could benefit from exploring adaptive learning mechanisms, enabling the system to dynamically adjust its parameters in response to changing IoT network conditions. Additionally, the integration of edge computing and blockchain technology could enhance security and further optimize resource allocation in the context of green communication. Finally, the scalability and applicability of the CEOGC-DLLP model to diverse IoT use cases and network architectures should be thoroughly investigated to ensure its effectiveness in various real-world scenarios.

ACKNOWLEDGMENT

The authors extend their appreciation to the Deanship of Scientific Research at King Khalid University for funding this work through large group Research Project under grant number (RGP2/95/44). Princess Nourah bint Abdulrahman University Researchers Supporting Project number (PNURSP2023R203), Princess Nourah bint Abdulrahman

University, Riyadh, Saudi Arabia. Research Supporting Project number (RSP2023R459), King Saud University, Riyadh, Saudi Arabia. This study is supported via funding from Prince Sattam bin Abdulaziz University project number (PSAU/2023/R/1444). This study is partially funded by the Future University in Egypt (FUE).

REFERENCES

[1] P. Chithaluru, F. Al-Turjman, M. Kumar, and T. Stephan, "Energy-balanced neuro-fuzzy dynamic clustering scheme for green & sustainable IoT based smart cities," *Sustain. Cities Soc.*, vol. 90, Mar. 2023, Art. no. 104366.

[2] Z. Yan, Z. Sun, R. Shi, and M. Zhao, "Smart city and green development: Empirical evidence from the perspective of green technological innovation," *Technolog. Forecasting Social Change*, vol. 191, Jun. 2023, Art. no. 122507.

[3] M. A. Albreem, A. M. Sheikh, M. J. K. Bashir, and A. A. El-Saleh, "Towards green Internet of Things (IoT) for a sustainable future in Gulf cooperation council countries: Current practices, challenges and future prospective," *Wireless Netw.*, vol. 29, no. 2, pp. 539–567, Feb. 2023.

[4] A. Oad, H. G. Ahmad, M. S. H. Talpur, C. Zhao, and A. Pervez, "Green smart grid predictive analysis to integrate sustainable energy of emerging V2G in smart city technologies," *Optik*, vol. 272, Feb. 2023, Art. no. 170146.

[5] S. T. Ahmed, S. M. Basha, M. Ramachandran, M. Daneshmand, and A. H. Gandomi, "An edge-AI enabled autonomous connected ambulance route resource recommendation protocol (ACA-R3) for eHealth in smart cities," *IEEE Internet Things J.*, to be published.

[6] S. Popli, R. K. Jha, and S. Jain, "Green IoT: A short survey on technical evolution & techniques," *Wireless Pers. Commun.*, vol. 123, no. 1, pp. 525–553, Mar. 2022.

[7] A. Mukherjee, P. Goswami, L. Yang, Z. Yan, and M. Daneshmand, "Dynamic clustering method based on power demand and information volume for intelligent and green IoT," *Comput. Commun.*, vol. 152, pp. 119–125, Feb. 2020.

[8] S. H. Alsamhi, F. Afghah, R. Sahal, A. Hawbani, M. A. A. Al-qaness, B. Lee, and M. Guizani, "Green Internet of Things using UAVs in B5G networks: A review of applications and strategies," *Ad Hoc Netw.*, vol. 117, Jun. 2021, Art. no. 102505.

[9] Z. Du, "Energy analysis of Internet of Things data mining algorithm for smart green communication networks," *Comput. Commun.*, vol. 152, pp. 223–231, Feb. 2020.

[10] P. K. R. Maddikunta, T. R. Gadekallu, R. Kaluri, G. Srivastava, R. M. Parizi, and M. S. Khan, "Green communication in IoT networks using a hybrid optimization algorithm," *Comput. Commun.*, vol. 159, pp. 97–107, Jun. 2020.

[11] K. Dev, P. K. R. Maddikunta, T. R. Gadekallu, S. Bhattacharya, P. Hegde, and S. Singh, "Energy optimization for green communication in IoT using Harris hawks optimization," *IEEE Trans. Green Commun. Netw.*, vol. 6, no. 2, pp. 685–694, Jun. 2022.

[12] S. Verma, S. Kaur, M. A. Khan, and P. S. Sehdev, "Toward green communication in 6G-enabled massive Internet of Things," *IEEE Internet Things J.*, vol. 8, no. 7, pp. 5408–5415, Apr. 2021.

[13] M. M. Akhtar, D. Ahamad, A. E. M. Abdalrahman, A. S. A. Shatat, and A. S. A. Shatat, "A novel hybrid meta-heuristic concept for green communication in IoT networks: An intelligent clustering model," *Int. J. Commun. Syst.*, vol. 35, no. 6, Apr. 2022, Art. no. e5089.

[14] S. Singh, A. S. Nandan, A. Malik, R. Kumar, L. K. Awasthi, and N. Kumar, "A GA-based sustainable and secure green data communication method using IoT-enabled WSN in healthcare," *IEEE Internet Things J.*, vol. 9, no. 10, pp. 7481–7490, May 2022.

[15] A. Rehman, K. Haseeb, T. Saba, and H. Kolivand, "M-SMDM: A model of security measures using green Internet of Things with cloud integrated data management for smart cities," *Environ. Technol. Innov.*, vol. 24, Nov. 2021, Art. no. 101802.

[16] S. Kumar, O. Kaiwartya, M. Rathee, N. Kumar, and J. Lloret, "Toward energy-oriented optimization for green communication in sensor enabled IoT environments," *IEEE Syst. J.*, vol. 14, no. 4, pp. 4663–4673, Dec. 2020.

[17] G. Kaur, P. Chanak, and M. Bhattacharya, "A green hybrid congestion management scheme for IoT-enabled WSNs," *IEEE Trans. Green Commun. Netw.*, vol. 6, no. 4, pp. 2144–2155, Dec. 2022.

[18] H. Zhang, F. Zhang, B. Gong, X. Zhang, and Y. Zhu, "The optimization of supply chain financing for bank green credit using Stackelberg game theory in digital economy under Internet of Things," *J. Organizational End User Comput.*, vol. 35, no. 3, pp. 1–16, Feb. 2023.

[19] V. B. Emroozi, P. Roozkhosh, A. Modares, and F. Roozkhosh, "Selecting green suppliers by considering the Internet of Things and CMCDM approach," *Process Integr. Optim. Sustainability*, vol. 7, no. 5, pp. 1167–1189, Nov. 2023.

[20] T. Zhang, P. Ren, D. Xu, and Z. Ren, "RIS subarray optimization with reinforcement learning for green symbiotic communications in Internet of Things (IoT)," *IEEE Internet Things J.*, to be published.

[21] G. Alandjani, "Integrating AI with green Internet of Things in healthcare for achieving UN's SDGs," *Tuijin Jishu/J. Propuls. Technol.*, vol. 44, no. 3, pp. 513–521, Jul. 2023.

[22] A. Faramarzi, M. Heidarinejad, B. Stephens, and S. Mirjalili, "Equilibrium optimizer: A novel optimization algorithm," *Knowl.-Based Syst.*, vol. 191, Mar. 2020, Art. no. 105190.

[23] B.-C. Yu and L.-S. Shao, "Optimization of the non-stop switchover system control for the main fans used in mining applications," *Mech. Ind.*, vol. 23, p. 25, Jan. 2022.

[24] S. K. Chaurasiya, A. Biswas, P. K. Bandyopadhyay, A. Banerjee, and R. Banerjee, "Metaheuristic load-balancing-based clustering technique in wireless sensor networks," *Wireless Commun. Mobile Comput.*, vol. 2022, pp. 1–21, Jan. 2022.

[25] J. Yan and X. Ma, "Microblog emotion analysis method using deep learning in spark big data environment," *Mobile Inf. Syst.*, vol. 2022, pp. 1–9, Aug. 2022.